

Evidence for Orbital-Specific Electron Transfer to Oriented Haloform Molecules

Beike Jia, Jonathan Laib, R. F. M. Lobo,[†] and Philip R. Brooks*

Contribution from the Chemistry Department and Rice Quantum Institute, Rice University, Houston, Texas 77251

Received July 15, 2002

Abstract: Beams of hyperthermal K atoms cross beams of the oriented haloforms CF₃H, CCl₃H, and CBr₃H, and transfer of an electron mainly produces K⁺ and the X⁻ halide ion which are detected in coincidence. As expected, the steric asymmetry of CCl₃H and CBr₃H is very small and the halogen end is more reactive. However, even though there are three potentially reactive centers on each molecule, the F⁻ ion yield in CF₃H is strongly dependent on orientation. At energies close to the threshold for ion-pair formation (~5.5 eV), H-end attack is more reactive to form F⁻. As the energy is increased, the more productive end switches, and F-end attack dominates the reactivity. In CF₃H near threshold the electron is apparently transferred to the σ_{CH}^* antibonding orbital, and small signals are observed from electrons and CF₃⁻ ions, indicating "activation" of this orbital. In CCl₃H and CBr₃H the steric asymmetry is very small, and signals from free electrons and CX₃⁻ ions are barely detectable, indicating that the σ_{CH}^* antibonding orbital is not activated. The electron is apparently transferred to the σ_{CX}^* orbital which is believed to be the LUMO. At very low energies the proximity of the incipient ions probably determines whether salt molecules or ions are formed.

Introduction

Direct experiments with oriented reagents show what had been surmised for a long time: chemical processes depend on the reagent orientation. These processes include chemical reaction,^{1,2} electron transfer,^{3,4} ionization,⁵ photodissociation,⁶⁻⁹ energy transfer,^{10,11} and surface scattering.^{10,12,13} Relatively small molecules have been oriented by "brute force" techniques,^{14,15} and a number of small symmetric tops have been studied by selecting orientations using an inhomogeneous electric field.^{1,2}

* To whom correspondence should be addressed. E-mail: brooks@python.rice.edu.

[†] Permanent address: Grupo de Nanotecnologia e Ciência à Nano-Escala, Departamento de Física, Faculdade de Ciência e Tecnologia, Universidade Nova de Lisboa, Monte Caparica, Portugal.

- (1) Loesch, H. J. *Annu. Rev. Phys. Chem.* **1995**, *46*, 555-94.
- (2) Parker, D. H.; Bernstein, R. B. *Annu. Rev. Phys. Chem.* **1989**, *40*, 561-595.
- (3) Brooks, P. R. *Int. Rev. Phys. Chem.* **1995**, *14*, 327-354.
- (4) Brooks, P. R.; Harland, P. W. *Effect of Molecular Orientation on Electron Transfer and Electron Impact Ionization*; Adams, N. G., Babcock, L. M., Eds.; JAI Press: Greenwich, CT, 1996; Vol. 2, pp 1-39.
- (5) Aitken, C. G.; Blunt, D. A.; Harland, P. W. *J. Chem. Phys.* **1994**, *101*, 11074-76.
- (6) Gandhi, S. R.; Curtiss, T. J.; Bernstein, R. B. *Phys. Rev. Lett.* **1987**, *59*, 2951-2954.
- (7) Fuglesang, C. D.; Baugh, D. A.; Pipes, L. C. *J. Chem. Phys.* **1996**, *105*, 9796.
- (8) Janssen, M. H. M.; Mastenbroek, J. W. G.; Stolte, S. *J. Phys. Chem. A* **1997**, *101*, 7605-13.
- (9) Castle, K. J.; Kong, W. *J. Chem. Phys.* **2000**, *112*, 10156-61.
- (10) Ionov, S. I.; LaVilla, M. E.; Mackay, R. S.; Bernstein, R. B. *J. Chem. Phys.* **1990**, *93*, 7406-15.
- (11) vanBeek, M. C.; terMeulen, J. J. *J. Chem. Phys.* **2001**, *115*, 1843-52.
- (12) Lahaye, R. J. W. E.; Stolte, S.; Holloway, S.; Kleyn, A. W. *J. Chem. Phys.* **1996**, *104*, 8301-8311.
- (13) Tenner, M. G.; Kuipers, E. W.; Kleyn, A. W.; Stolte, S. *J. Chem. Phys.* **1988**, *89*, 6552-53.
- (14) Loesch, H. J.; Remscheid, A. *J. Chem. Phys.* **1990**, *93*, 4779-4790.
- (15) Friedrich, B.; Herschbach, D. R. *Z. Phys.* **1991**, *D18*, 153.

Although the effects of orientation are real, the magnitude of the steric asymmetries observed thus far has been comparatively small, especially since our mental picture of reaction is usually that of an "all-or-nothing" process. Our imagination, however, paints a classical picture of a molecule fixed in space and fails to account for a quantal distribution of orientations that must result even from a single quantum state. Likewise, the experiments have failed to produce a highly oriented sample, either because hard-to-orient high *J* states are present in the brute force experiments or because hard-to-orient prolate symmetric tops have been (mainly) used in the hexapole selection experiments.

We have chosen to study the haloform molecules, not only because of their role in atmospheric reactions¹⁶ and their implication in global warming¹⁷ but also for their intrinsic interest. Whereas most small molecules are near-prolate tops¹⁸ which are difficult to spin about their symmetry axes, these molecules, CF₃H, CCl₃H, and CBr₃H, are all oblate tops and rotate like a bicycle wheel. They should produce a distribution of orientations closer to our mental picture than does a prolate top such as CH₃Br. But since they have three potentially reactive sites and since the H atom is usually considered insignificant, we expected that the steric asymmetry might still be small. This is true for CCl₃H and CBr₃H. To our great surprise, however,

- (16) *Scientific Assessment of Ozone Depletion*; National Oceanic and Atmospheric Administration: Washington, DC, and World Meteorological Organization: Geneva, Switzerland, 1999.
- (17) Albritton, D. L.; Filho, L. G. M. *Climate Change 2001: The Scientific Basis: Contribution of Working Group I to the Third Assessment Report of the Intergovernmental Panel on Climate Change*; Houghton, J. T., Ding, Y., Griggs, D. J., Noguer, M., van der Linden, P. J., Dai, X., Maskell, K., Johnson, C. A., Eds.; Cambridge University Press: New York, 2001.
- (18) Kinsey, J. L.; Silbey, R. J. *J. Chem. Phys.* **1988**, *88*, 4100-1.

not only is the steric asymmetry of CF_3H larger than any molecule we have examined, but the steric asymmetry also changes sign as the collision energy is changed. At energies near the threshold for ion-pair production (~ 5.5 eV) F^- is produced preferentially by attack at the H-end of the molecule. As the energy is raised, the preference shifts to the CF_3 -end, and the asymmetry maximizes and then declines. This behavior appears to arise from a low-energy reaction channel favored by H-end attack and a higher-energy channel favored by CF_3 -end attack. At low energies the electron is most likely transferred to the σ_{CH}^* orbital at the H-end of the molecule, but at higher energies the preference apparently shifts to the σ_{CF}^* at the F-end of the molecule.

Experimental Section

The experimental apparatus has been previously described.^{19,20} A beam of fast (4–30 eV) K atoms produced by charge exchange²¹ intersects a beam of hexapole state-selected molecules between two small time-of-flight (TOF) mass spectrometers identical except for polarity. The beams are continuous, and the voltages on the mass spectrometers are constant so that there is no time zero. Since the positive and negative ions are produced simultaneously, the *difference* in flight times provides mass analysis as long as the count rate is low enough to avoid confusing ions from different events.

Halofrom beams were produced from 10% mixtures in helium except for bromoform, which was produced by passing 150 Torr of helium over liquid CBr_3H at ~ 22 °C (vapor pressure ~ 6 Torr) making the beam about 4% in CBr_3H . Signal fluctuations apparently caused by variations in surface area at the liquid–gas interface were minimized with a fiberglass wick which increased the surface area and greatly stabilized the signal.

An inhomogeneous hexapole electric field selects molecules in well-defined quantum states. The beam is coaxial with the rods, and molecules are deflected in this field according to their rotational state described by the quantum numbers J , K , and M .²² The interaction energy of the top with the electric field is given by

$$W = -\mu \cdot E = -\mu EMK/(J(J+1)) = -\mu E \langle \cos \theta \rangle \quad (1)$$

where θ is the angle between the top axis and the electric field. For molecules with $\langle \cos \theta \rangle > 0$, the energy decreases as the field increases, and molecules in these quantum states will be drawn toward the charged rods of the hexapole and are defocused. Molecules with $\langle \cos \theta \rangle < 0$ are *focused* by being forced toward the axis where the field is zero; the beam intensity increases when voltage is applied to the rods. Those with $\langle \cos \theta \rangle = 0$ are unaffected.

The beam of molecules leaves the state-selecting field, passes through an aperture, and enters an ultrahigh vacuum collision chamber where the molecules intersect the beam of fast K atoms. Collisions occur in a weak (~ 300 V/cm) electric field between the two TOF mass spectrometers. (A weak electric field is present along the molecule flight to ensure that the molecules remain in the same J , K , and M states.) Molecules in these selected quantum states are *oriented* with respect to the field between the mass spectrometers.²³ If the polarities of the mass spectrometers are reversed, the field direction between them is reversed, and the laboratory orientation of the molecules is also reversed. The molecules always remain in quantum states with $\langle \cos \theta \rangle < 0$, corresponding to the negative end of the molecule pointing toward the negatively charged field plate.

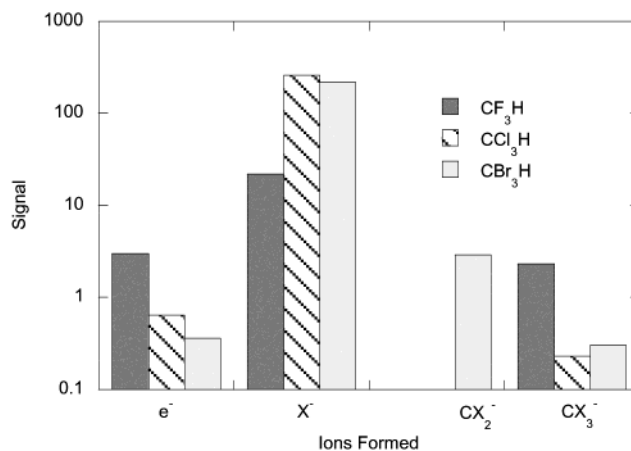


Figure 1. Comparison of ion signals among the haloforms studied at 10 eV CM. The relative cross section of CBr_3H is about $2.5\times$ larger than suggested in the figure.

The polarities of the TOF mass spectrometers determine whether the positive or negative end of the molecule is attacked, and data are taken for each of these polarities with the hexapole field energized and with the hexapole field off. The hexapole field does not have a beam stop so that when the hexapole is not energized a weak, *totally random* beam is transmitted. The signals from symmetric top molecules increase when the high voltage (HV) is applied which helps to identify the mass peaks for calibration. The steric asymmetry is calculated from the $\text{HV}_{\text{on}} - \text{HV}_{\text{off}}$ difference, ΔS_{\pm} , (\pm denotes positive- or negative-end attack), and the random beam signals are used to eliminate differences in collection efficiency or detection efficiency, which arise when the detector polarities are reversed.²⁴ A computer turns the HV on and off for each orientation at a given collision energy to rapidly compare orientations. The collision energy sequence is chosen randomly and differs from day to day.

This coincidence TOF mass spectrometer system collects ions from an extensive volume using the Wiley–McLaren²⁵ technique to space-focus the ions. But the flight time depends on the initial kinetic energy of the neutral reagents because the extraction field is nominally parallel or antiparallel to the large relative velocity. There is thus a considerable shift between the flight times for positive-end or negative-end attack, and the spread in relative velocities limits the resolution¹⁹ to about 2 amu at $m/e = 80$, which is insufficient to distinguish between CF_3^- and CF_3H^- .

For CCl_3H only the $^{35}\text{Cl}^-$ signals were analyzed because simultaneous electrical interference impressed on both channels appears near mass 39. To a first approximation, this interference is identical with HV_{on} and HV_{off} and the difference is zero, but small fluctuations can swamp nearby real signals.

Results

Electron transfer to the various haloforms mainly produces the halide ion, although free electrons and anions with m/e near that of CX_3^- are formed in small abundance. Figure 1 shows representative relative ion signals at 10 eV for the three molecules. The relative cross section for CBr_3H is about 2.5 times larger than suggested by Figure 1 because, as previously described, helium passed over the liquid to form the CBr_3H beam. Although our mass resolution cannot distinguish between even CF_3^- and CF_3H^- , these ions (and those from CCl_3H and CBr_3H) are thought to be CX_3^- on the basis of their thresholds and electron affinities.^{26,27} For CBr_3H an ion with $m/e \approx 172$ appears which could be either CBr_2H^- or CBr_2^- resulting from

(19) Harris, S. A.; Wiediger, S. D.; Brooks, P. R. *J. Phys. Chem.* **1999**, *103*, 10035–41.

(20) Harris, S. A.; Harland, P. W.; Brooks, P. R. *Phys. Chem. Chem. Phys.* **2000**, *2*, 787–91.

(21) Helbing, R. K. B.; Rothe, E. M. *Rev. Sci. Instrum.* **1968**, *39*, 1948.

(22) Townes, C. H.; Schawlow, A. L. *Microwave Spectroscopy*; Dover: New York, 1975.

(23) Brooks, P. R.; Jones, E. M.; Smith, K. *J. Chem. Phys.* **1969**, *51*, 3073.

(24) Brooks, P. R.; Harris, S. A. *J. Chem. Phys.* **2002**, *117*, 4220–32.

(25) Wiley, W. C.; McLaren, I. H. *Rev. Sci. Instr.* **1955**, *26*, 1150.

Table 1. Apparent Thresholds (Predicted^{26,27,30})

molecule	electrons	X ⁻	CX ₂ ⁻	CX ₃ ⁻
CF ₃ H	6.7 ± 0.4 (4.34)	5.8 ± 0.4 (5.6)		7.1 ± 0.4 (6.9)
CCl ₃ H	6.7 ± 0.3 (4.34)	4.6 ± 0.2 (4.2)		6.0 ± 0.5 (6.1)
CBr ₃ H	6.2 ± 0.3 (4.34)	4.0 ± 0.2 (3.7)	4.5 ± 0.3 (~5.3 CHBr ₂ ⁻) (~6 CBr ₂ ⁻) (~9.8 CBr ₂ ⁻ + H + Br)	5.2 ± 0.53 (~7)

loss of a Br atom or an HBr molecule. We are unable to distinguish between these ions.

Threshold Energies. Nominal threshold energies are shown in Table 1. The energy scale was calibrated with SF₆.²⁸ These apparent thresholds are rather rough values, given our inability to account for the energy spread in the K atom beam and the spread in the data due to day-to-day fluctuations in absolute intensity. The X⁻ thresholds are comparable to those expected and are the same for both orientations. The electron thresholds seem uniformly high by more than about 2 eV. This suggests that the molecules may be intimately involved in a sequential process in which a transient molecular negative ion is formed for a short time before the electron is ejected and that the molecule is left in a state excited by some 2 eV after the electron departs. The apparent threshold for “CBr₃” is ~1.8 eV less than predicted,^{27,26} suggesting that either the EA for CBr₃ is much larger or that this ion may correspond to the parent negative ion, CHBr₃⁻ which has been predicted to be stable.²⁹

Steric Effects. The experimental signal rates for positive-end and negative-end attack depend strongly on energy because the K beam intensity and the cross section both increase strongly with energy.³¹ To focus on the steric effects, this variation is removed by defining the *steric asymmetry* $G(E)$ in terms of the cross sections for positive-end attack, $\sigma_+(E)$ and negative-end attack, $\sigma_-(E)$ as

$$G(E) = \frac{(\sigma_-(E) - \sigma_+(E))}{(\sigma_-(E) + \sigma_+(E))} \quad (2)$$

This is obtained from the experimental signal differences $\Delta S_{\pm}(E)$ and ratios $R_{\pm}(E)$,²⁴ where $S_{\pm}(E, V)$ is the experimental signal for positive- or negative-end attack at energy E and hexapole voltage V . The steric asymmetry $G(E)$ is zero if the positive-end and negative-end reactivities are the same and becomes ± 1 if only one end is reactive, depending on the polarity of the reactive end.

Halide Ions. The steric asymmetry for formation of halide ions is shown in Figure 2. Even though there are three potentially reactive sites, G for CF₃H is the largest we have measured and clearly reverses sign as the energy is changed. At low energies *positive*-end attack favors the formation of F⁻. The asymmetry

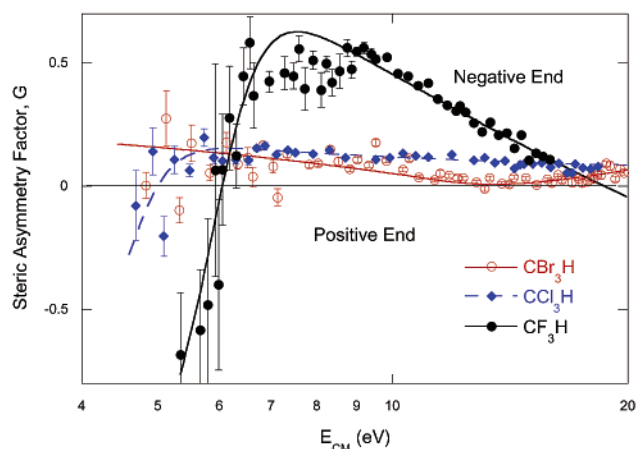


Figure 2. Steric asymmetry for formation of halide ions, X⁻ for the three haloforms. Error bars are $\pm 1\sigma$, and curves are model fits to the data. A log scale is used to better display the low-energy data.

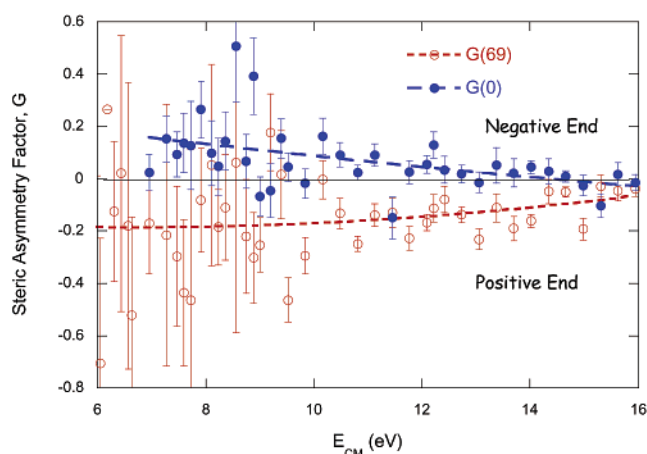


Figure 3. Steric asymmetry for electrons and CF₃⁻ ions formed after electron transfer to fluoroform. Least-squares quadratic fits are drawn to distinguish the electron asymmetry from the CF₃⁻ asymmetry.

changes sign near 6 eV, whereupon negative-end attack is more favorable. The asymmetry maximizes in the 7–9 eV range and then declines. That for chloroform might be similar, but the effect is far less dramatic. Bromoform reacts almost as if it were spherical, with only a slight preference for negative-end attack. The asymmetry for CBr₃H is extremely small and appears to minimize near 15 eV.

Data were taken over many months, and the absolute signal rates are subject to fluctuations from beam-intensity variations. These fluctuations affect the threshold values but are less severe for G values. As a consequence, a few G values are included for energies below the rough thresholds given in Table 1. The G values are deemed more reliable than the thresholds.

Electrons and CX₃⁻ Ions. Other ions are formed in much lower abundance, as shown in Figure 1, and the steric asymmetry is more difficult to measure, especially at low energies. Figure 3 shows data for fluoroform. Electrons seem to be preferentially formed upon negative-end attack. Although the data for CF₃⁻ is noisy at low energies, the trend is opposite to that for the electrons, and formation of CF₃⁻ is favored for positive-end attack.

Figure 4 shows the steric asymmetry for electrons and for CCl₃⁻ ions from chloroform. The data seems rather scattered, but very broadly speaking, the steric asymmetry shows the same

(26) Lias, S. G.; Bartmess, J. E.; Liebman, J. F.; Holmes, J. L.; Levin, R. D.; Mallard, W. G. *J. Phys. Chem. Ref. Data* **1988**, *17*, Supplement 1.

(27) Deyerl, H. J.; Alconcel, L. S.; Continetti, R. E. *J. Phys. Chem* **2001**, *105*, 552–7.

(28) Harris, S. A.; Brooks, P. R. *J. Chem. Phys.* **2001**, *114*, 10569–72.

(29) Modelli, A.; Scagnolari, F.; Distefano, G.; Jones, D.; Guerra, M. *J. Chem. Phys.* **1992**, *96*, 2061–70.

(30) Kerr, J. A.; Stocker, D. W. *Handbook of Chemistry and Physics*; CRC Press: Boca Raton, FL, 2000.

(31) Xing, G.; Kasai, T.; Brooks, P. R. *J. Am. Chem. Soc.* **1995**, *117*, 2581–2589.

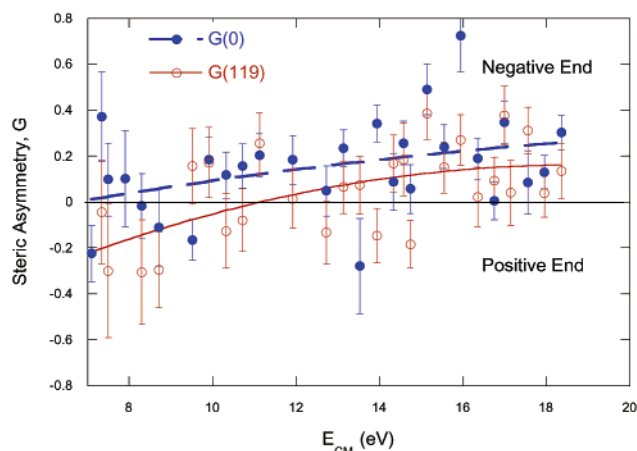


Figure 4. Steric asymmetry for electrons and CCl_3^- ions from CCl_3H . The curves are least-squares quadratic fits drawn to compare the behavior of the two ions.

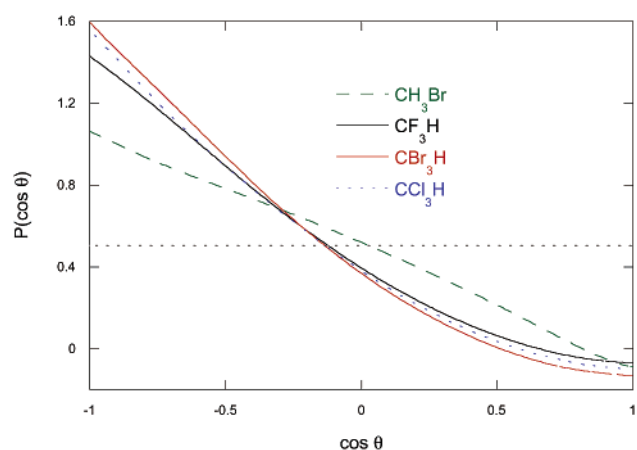


Figure 5. Calculated $\text{HV}_{\text{on}} - \text{HV}_{\text{off}}$ probability distributions for CF_3H , CCl_3H , and CBr_3H . The CH_3Br distribution is shown for comparison. The dotted horizontal line is obtained for a random sample. The $\text{HV}_{\text{on}} - \text{HV}_{\text{off}}$ difference characterizes a sample richer in “correctly” oriented molecules (those with $\langle \cos \theta \rangle \sim -1$) and poorer in “wrongly” oriented molecules.

trend as for CF_3H . Negative-end attack seems to produce more electrons, and positive-end attack, more CCl_3^- . The analogous data for bromoform is highly scattered and is not shown.

Comparison of Orientation Distributions. Figure 2 shows not only an enormous steric effect for CF_3H but also a remarkable difference between the very asymmetric reactivity of CF_3H and the nearly spherical behavior of CCl_3H and CBr_3H . To determine if this is a result of an intrinsic difference in reactivity between CF_3H and the heavier haloforms or is a consequence of CF_3H being better oriented, we compared the orientation distributions for the molecules.

Rather than being perfectly oriented, the molecules are distributed in an array of quantum states, each molecule having $\langle \cos \theta \rangle < 0$. The probability of the molecular axis being oriented within a narrow angular range is given by^{32–34}

$$P(\cos \theta) = \sum_J \sum_{K=-J}^J \sum_{M=-J}^J P_{JKM}(\cos \theta) f_{JK}(T) F_{JKM}(V) \quad (3)$$

(32) Stolte, S. *Ber. Bunsen-Ges. Phys. Chem* **1982**, *86*, 413–421.

(33) Stolte, S.; Chakravorty, K. K.; Bernstein, R. B.; Parker, D. H. *Chem Phys* **1982**, *71*, 353–361.

(34) Choi, S. E.; Bernstein, R. B. *J. Chem. Phys.* **1986**, *85*, 150–161.

which is the overall sum of the quantum probability distribution function, $P_{JKM}(\cos \theta)$, weighted by $f_{JK}(T)$, the fraction of molecules in states J, K at temperature T , and weighted by $F_{JKM}(V)$, the probability of being transmitted through the field at voltage V .

The distribution calculated from eq 3 accounts for molecules in states with $\langle \cos \theta \rangle < 0$ being focused, for those in states with $\langle \cos \theta \rangle > 0$ being defocused, and for those in states with $\langle \cos \theta \rangle = 0$ being unaffected but in divergent trajectories. The distribution for a random beam, $P(\cos \theta) = 0.5$, is subtracted to give $P(\cos \theta)$ appropriate for ΔS_{\pm} . Figure 5 shows the normalized difference distribution for ΔS_{\pm} . Well-oriented molecules ($\langle \cos \theta \rangle \sim -1$) are enhanced, and poorly oriented molecules ($\langle \cos \theta \rangle \sim +1$) are diminished in comparison to a randomly oriented sample (dotted horizontal line in Figure 5). The probability distributions are well fit by a truncated expansion in Legendre polynomials,³³

$$P(\cos \theta) = \sum_{i=0}^3 a_i P_i(\cos \theta) \quad (4)$$

and these coefficients are given in Table 2.

Figure 5 shows that the haloforms are oriented, that they are much better oriented than CH_3Br , and that the orientation distributions for the haloforms are qualitatively similar. But CF_3H is *not* as well oriented as CCl_3H or CBr_3H , even though Figure 2 shows that the steric asymmetry is much larger for CF_3H . We are thus forced to conclude that the intrinsic steric asymmetry for CF_3H is much larger than that for either CCl_3H or CBr_3H .

Models. Previous experiments^{24,28} on CH_3Br and *t*- $\text{C}_4\text{H}_9\text{Br}$ showed trends in the steric asymmetry similar to that shown here for CF_3H . Those data could be represented by a model in which reaction occurred via two competing mechanisms, one at low energy favoring CH₃-end approach, and the other at higher energy favoring Br-end approach. A similar model fits the steric asymmetry of Figure 2. For energies greater than a high threshold, E_{H} , the orientation-dependent cross section, σ_{\pm}^{H} , is (in relative units),

$$\begin{aligned} \sigma_{\pm}^{\text{H}} &= 0 \quad E \leq E_{\text{H}} \\ \sigma_{\pm}^{\text{H}} &= a_{\pm}^{\text{H}}(E - E_{\text{H}}) + b_{\pm}^{\text{H}}(E - E_{\text{H}})^2 \quad E > E_{\text{H}} \end{aligned} \quad (5)$$

The low-energy cross section is assumed to have the same form with a lower threshold, E_{L} , but attenuated exponentially with constant c as a consequence of the opening of the higher-energy channel,

$$\begin{aligned} \sigma_{\pm}^{\text{L}} &= 0 \quad E \leq E_{\text{L}} \\ \sigma_{\pm}^{\text{L}} &= a_{\pm}^{\text{L}}(E - E_{\text{L}}) + b_{\pm}^{\text{L}}(E - E_{\text{L}})^2 \quad E_{\text{H}} > E > E_{\text{L}} \\ \sigma_{\pm}^{\text{L}} &= (a_{\pm}^{\text{L}}(E - E_{\text{L}}) + b_{\pm}^{\text{L}}(E - E_{\text{L}})^2) e^{-c(E - E_{\text{H}})} \quad E > E_{\text{H}} \end{aligned} \quad (6)$$

where a_{\pm}^{H} and b_{\pm}^{H} are adjustable parameters for the positive and negative attack orientations. The overall cross section is $\sigma_{\pm} = \sigma_{\pm}^{\text{L}} + \sigma_{\pm}^{\text{H}}$.

Table 2. Legendre Coefficients for $P(\cos \theta)$

	a_1	a_2	a_3
CF ₃ H	-0.796	0.197	0.041
CCl ₃ H	-0.846	0.232	0.016
CBr ₃ H	-0.902	0.246	0.038
CH ₃ Br	-0.578	-0.034	-0.006
<i>t</i> -C ₄ H ₉ Br	-0.641	0.027	0.011

Table 3. Model Cross Section Parameters^a

	Br (<i>t</i> -C ₄ H ₉ Br) ²⁴	CF ₃ H	CCl ₃ H	CBr ₃ H
E_H	4.35	5.2	3.0	11
E_L	4.05	4.05	1.5	1.5
a_-^H	250	2000	70	2.7
b_-^H	27	5	20	7
a_+^H	40	40	40	2.6
b_+^H	40	150	18	4
a_-^L	100	100	100	28
b_-^L	100	100	100	0.05
a_+^L	1500	1500	1500	20
b_+^L	2000	2000	2000	0.8
c	5	2.2	3	0.01

^a E is measured in eV; others are (eV)⁻¹ or (eV)⁻² to make σ dimensionless.

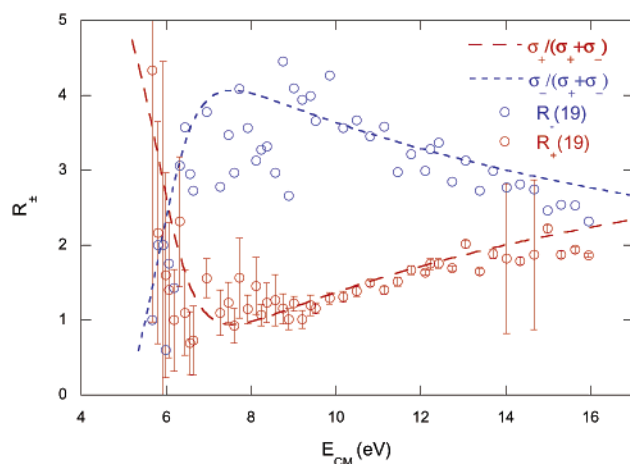


Figure 6. Experimental values of $R_{\pm}(E)$ for F^- ions from CF_3H compared with model fits using the parameters found by fitting the steric asymmetry, G . All experimental error bars are shown for positive-end attack although some are smaller than the symbols. Error bars are comparable for negative-end attack but are omitted for clarity.

The parameters shown in Table 3 have been chosen on a trial-and-error basis to fit the steric asymmetry shown in Figure 2 and show that a reasonable model can fit the CF_3H steric asymmetry. Although these parameters are too numerous to fit, we note that they also fit the *separate* measurements of positive-end and negative-end reactivity from which G is derived. Figure 6 shows $R_{\pm}(E)$, the ratio of signals in a specific (\pm) orientation divided by the signal from random molecules, $S_{\pm}(E,0)$. The model comparison is $\sigma_{\pm}/(\sigma_+ + \sigma_-)$ scaled vertically at *one* point to fit the experimental data since the random orientation is not modeled but is present experimentally. This agreement provides reasonable confirmation of the model and fit for CF_3H .

The asymmetry for CBr_3H in Figure 2 shows a small minimum near 15 eV. This minimum is probably due to a competition between reaction channels which both favor attack at the CBr_3 -end, but this cannot be confirmed by the present data.

Discussion

Orbital Differences. The data shown in Figure 2 demonstrate that there is an enormous steric effect for CF_3H . Attacking the positive end produces more F^- just above the ion production threshold, and this preference rapidly shifts to the negative end as the energy increases. On the other hand, the steric asymmetry for CCl_3H and CBr_3H is almost negligible. Any hindering effect of the hydrogen atom would be expected to be about equally effective in each of the haloforms, and hindrance cannot account for the H-end reactivity in CF_3H . Clearly, factors other than shielding by the H atom are important here, and we believe that the electronic structure of the molecule plays a prominent role.

Fluoroform is known to be qualitatively different from the heavier haloforms. Although the CH bond is generally stronger than the CX bond, the opposite is true in CF_3H where the dissociation energy³⁰ of the CF bond is 4.8–5.4 eV compared to 4.67 for the CH bond. The optical spectra of fluoroform differs from that of the other haloforms in that the lower-energy Rydberg transitions appear to originate from alkyl group orbitals rather than from the halogen lone pairs.³⁵ The HOMO in CF_3H is largely the σ_{CH} orbital,³⁶ and the lowest-lying σ^* orbitals are largely centered on the C atom.²⁹

The steric data of Figures 2 and 6 are fit reasonably well by the model, suggesting that low-energy reaction occurs mainly at the H-end of the molecule. This channel is attenuated in favor of a more likely channel opening at higher energy but favoring the CF_3 -end of the molecule. Similar, but less pronounced, behavior was previously observed for electron transfer to CH_3Br and $t-C_4H_9Br$ ^{24,28} where it was suggested that the electron could be transferred into different orbitals of the molecule, depending on the orientation and energy. Near the threshold for ion-pair formation only the LUMO is energetically accessible, but higher-lying orbitals could become accessible as the energy is increased.

Thus, for CF_3H at energies near threshold an electron will enter the LUMO which is most likely a σ_{CH}^* orbital with lobes extending in both directions along the C–H bond. The electron could be transferred into the LUMO at either lobe, to form a molecular negative ion with a charge distribution only partially described as σ_{CH}^* . The haloform negative molecular ions probably distribute the charge over the molecule in a state with σ_{CH}^* as well as σ_{CF}^* character. If a *free* electron were attached, the attachment process would be so rapid that the molecular ion would be formed in the geometry of the neutral. In contrast, transfer of a *bound* electron from a nearby atom introduces the possibility that the atomic ion could perturb the system during the process. Some aspect of the molecular geometry might change, but a negative molecular ion is still probably born in the geometry close to that of the neutral. Since the stable negative molecular ion would be expected to have elongated C–F bonds, the incipient ion formed here is most likely born with compressed C–F bonds. The compressed negative molecular ion is thus likely to dissociate to give an F^- ion.

The K^+ and F^- ions will be easier to separate if they are far apart, suggesting that observation of the charges will be facilitated by attack of the σ_{CH}^* lobe at the H-end of the

(35) Robin, M. B. *Higher Excited States of Polyatomic Molecules*; Academic Press: New York, 1974; Vol. 1.

(36) Brundle, C. R.; Robin, M. B.; Basch, H. *J. Chem. Phys.* **1970**, *53*, 2196–2213.

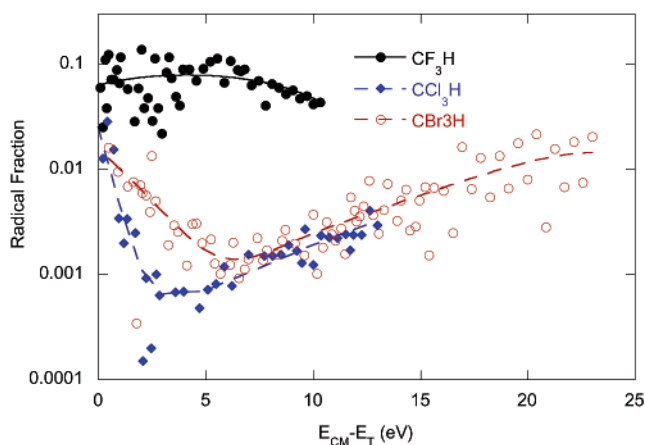


Figure 7. Fraction of signal due to CX_3^- ions for various haloforms as a function of energy above threshold for X^- formation. The curves are to guide the eye.

molecule. This could produce the incipient charges as far apart as possible. On the other hand, attack at the σ_{CH}^* lobe inside the CF_3 umbrella would leave the incipient charges close to one another, making it difficult to separate the charges at the very lowest energies, and the more likely result would be the formation of the salt KF . Since we only detect ions, formation of salt molecules would be interpreted as a diminished reactivity.

Transfer into the σ_{CH}^* lobe inside the umbrella becomes more likely to produce ions as the energy is raised. Also at higher energies the $C-F$ σ^* orbitals become accessible;³⁷ since there are three such orbitals, transfer into these orbitals could be almost orientation-independent, and the cross section would be much larger. The outcome of an electron-transfer collision thus depends not only on the energy and the accessibility of an unoccupied orbital but also on the relative proximity of the reagents.

For the heavier haloforms, exemplified by CCl_3H , the LUMO³⁸ is σ_{CX}^* , and electron transfer is more likely to occur to a peripheral σ_{CX}^* lobe rather than at the σ_{CH}^* lobe as in CF_3H . Thus, the cross section would be expected to be larger than that for CF_3H , and the steric asymmetry, smaller, as is observed. At energies near threshold, electron transfer to the σ_{CX}^* orbital located on one X atom would probably produce the salt KX , and this was detected in earlier experiments³⁹ on CCl_3H where the energy was too low to produce ions. The intensity and angular distribution of the salt product was independent of orientation, showing that there was no steric asymmetry. To produce the ions observed in the present experiments, it may be that the electron is transferred to a σ_{CX}^* orbital located on one X atom, followed by near-instantaneous rearrangement of the charge distribution to produce X^- at a more distant X atom. The separation of charges would facilitate their escape as ions.

The σ_{CH}^* orbital in CF_3H manifests itself in yet another way. In addition to the large difference in steric asymmetry between CF_3H and the heavier haloforms, as shown in Figure 2, there is also a major difference in the fragmentation pattern as suggested in Figure 1. This difference is shown in detail in Figure 7, where we plot the fraction of CX_3^- ions versus energy above the X^-

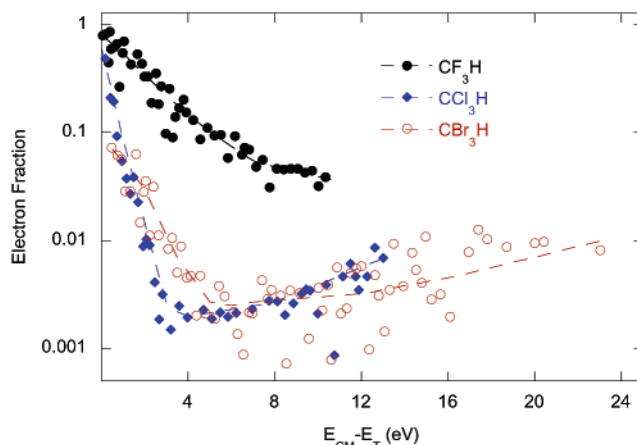


Figure 8. Fraction of electrons as a function of energy above threshold for X^- formation. The curves are to guide the eye.

threshold. Fluoroform is nearly 2 orders of magnitude more likely to produce CX_3^- than is either of the other two molecules. The electron fraction is similar and shown in Figure 8. Again this fraction is about 2 orders of magnitude larger in fluoroform. As previously discussed, an electron entering the σ_{CH}^* orbital would form a temporary negative molecular ion in a geometry close to that of the neutral. Even though the most likely result is breaking a $C-X$ bond, the CH bond could also break, or the electron could be ejected. Thus, a competition arises between autodetaching the electron and breaking either the $C-F$ or $C-H$ bond, and all of these processes occur in CF_3H . If the $C-H$ bond were tempted to break, the electron is more likely to be given to the CF_3 moiety, and CF_3^- ions are more likely to be formed if the alkali ion is far away at the H-end of the molecule, as shown in Figure 3. Likewise, formation of the free electron is favored by attack at the CF_3 -end. In the heavier haloforms the electron apparently does not enter the σ_{CH}^* orbital, the H-end is not reactive and according to the above mechanism does not produce either CX_3^- or electrons. Instead the electron likely enters the σ_{CX}^* orbital and the $C-X$ bond breaks, giving an X^- as the main product. In CBr_3H fission of the $C-Br$ bond may also produce CBr_2H^- as shown in Figure 1.

Models and Steric Factors. The complex steric asymmetry shown in Figure 2 defies a simple interpretation with a customary cone-of-reactivity model, but it is instructive to focus on the high-energy portion of the steric asymmetry where this model might apply. If reaction probability is one for approach within a cone of angle χ_0 and zero otherwise,²⁴ the calculated probability distributions of Figure 5 may be used to extract experimental estimates of χ_0 .^{3,4,24} For CF_3H near 8 eV this angle is near 120° and increases toward 180° as the energy is increased.

If χ_0 is known, the reaction model may be convoluted with the uniform probability distribution for a randomly oriented sample to give the gas-phase steric factor, ρ . This is the fraction of gas-phase collisions that have enough energy to react. As expected, the steric factors for CBr_3H and CCl_3H are nearly one, but those for CF_3H are noticeably lower than one. The minimum steric factor for CF_3H is ~ 0.7 which is similar to that for $t-C_4H_9Br$. (The steric asymmetry is larger for CF_3H , but it arises from a better oriented ensemble of molecules.) At high energies the steric factors have an Arrhenius-type of energy dependence as shown in Figure 9. The apparent steric “activation

(37) Varella, M. T. N.; Winstead, C.; McKoy, V.; Kitajima, M.; Tanaka, H. *Phys. Rev. A* **2002**, *65*, 22702–18.

(38) Ying, J. F.; Leung, K. T. *Phys. Rev. A* **1996**, *53*, 1476–86.

(39) Marcelin, G.; Brooks, P. R. *J. Am. Chem. Soc.* **1973**, *95*, 7885–6.

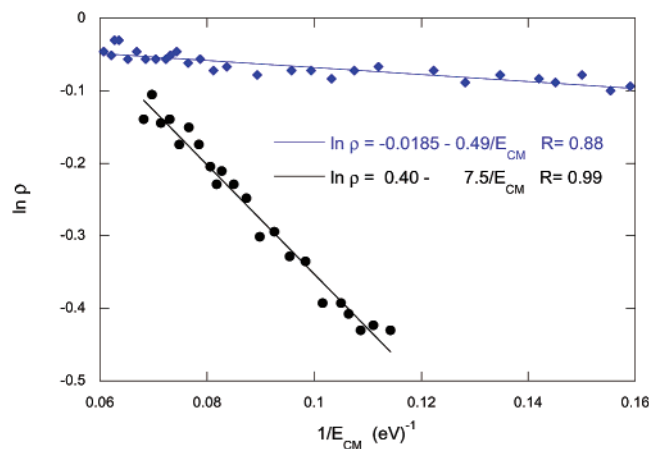


Figure 9. Arrhenius plot for the steric factor.

energies” are 7.5 and 0.5 eV for CF_3H and CCl_3H , respectively, which can be compared to 2.2 and 3.9 eV for CH_3Br and *t*- $\text{C}_4\text{H}_9\text{Br}$, respectively.²⁴

Summary

Electron transfer from K atoms to CF_3H , CCl_3H , and CBr_3H molecules oriented in space produce mainly the X^- halide ion and K^+ . The steric asymmetry for CCl_3H and CBr_3H is small as expected, and more X^- is produced by negative-end attack. Contrary to expectations, the steric asymmetry of CF_3H is large and changes with energy: at energies near the threshold for ion formation the H-end of the molecule is more reactive to form F^- , and this preference shifts to the CF_3 -end as the energy is increased.

The large differences between CF_3H and the two heavier haloforms is apparently a signature of different low-lying σ^* orbitals. The preference for H-end attack in CF_3H apparently arises from a low-lying σ^* orbital centered on the C or the CH bond, whereas the LUMO in the heavier haloforms is believed to be σ_{CX}^* , resulting in almost no steric preference. Occupation of the σ_{CH}^* orbital in CF_3H is apparently responsible for the formation of significantly more CF_3^- ions and free electrons than for the heavier haloforms.

Once the electron is transferred, the products formed, either ions or salt, depend on the proximity of the reactants as well as the energy. Formation of ions at very low energies is favored by “backside” attack where the incipient ions could be formed as far apart as possible. Close proximity favors salt formation which probably explains the lack of ion-pair formation for attack inside the CF_3 umbrella.

Classical steric factors, ρ , based on a cone-of-acceptance model are calculated from the experimental data and the theoretical distribution of orientations. The steric factors are close to one, and for CF_3H the minimum ρ is ~ 0.7 . At the higher energies the steric “activation energies” for CF_3H and CCl_3H are ~ 7.5 and 0.5 eV.

Acknowledgment. We gratefully acknowledge support for this research that has been received from the National Science Foundation and from the Robert A. Welch Foundation. R.F.M.L. thanks the ICCTI-Portugal for a sabbatical grant.

JA027710K